Spin evolution of radical pair with radical containing two groups of equivalent magnetic nuclei

V. A. Bagryansky
Institute of Chemical Kinetics & Combustion, Novosibirsk 630090, Russia and Novosibirsk State University, Novosibirsk 630090, Russia

K. L. Ivanov[a)]
Novosibirsk State University, Novosibirsk 630090, Russia and International Tomography Center, Novosibirsk 630090, Russia

V. I. Borovkov
Institute of Chemical Kinetics & Combustion, Novosibirsk 630090, Russia and Novosibirsk State University, Novosibirsk 630090, Russia

N. N. Lukzen
International Tomography Center, Novosibirsk 630090, Russia

Yu. N. Molin
Institute of Chemical Kinetics & Combustion, Novosibirsk 630090, Russia

(Received 25 January 2005; accepted 14 March 2005; published online 13 June 2005)

Analytical solution is obtained for time-resolved magnetic field effects (TR-MFE) on recombination fluorescence of radical-ion pair (RIP) containing radical ion with two groups of magnetically equivalent nuclei. The present theoretical approach is applied to three experimental systems: RIPs containing radical cations of 2,3-dimethylbutane, 2,2,6,6-tetramethylpiperidine, or diisopropylamine and radical anion of *p*-terphenyl-d_{14} in nonpolar alkane solutions. Good agreement between theory and experiment is found for all the three systems, hyperfine coupling constants of radical cations are obtained by fitting the experimental TR-MFE traces. The potential of the TR-MFE technique for studying radical ions with nonequivalent nuclei is discussed in detail. The wide applicability of the theoretical model and the experimental technique make them useful for studying short-lived radical species that are often beyond the reach of the conventional electron paramagnetic resonance spectroscopy. © *2005 American Institute of Physics*. [DOI: 10.1063/1.1901661]

I. INTRODUCTION

The method of time-resolved magnetic field effect (TR-MFE) in recombination fluorescence of spin-correlated radical ion pairs is a powerful tool for studying the properties of the short-lived radical ions formed under ionizing irradiation of nonpolar solutions.[1–12] As a rule, TR-MFE is defined as a ratio of recombination fluorescence kinetics in the presence and in the absence of external magnetic field. High temporal resolution of this experimental method that is about 1 ns allows one for studying elusive radical ion intermediates, which are often beyond the reach of the conventional electron paramagnetic resonance (EPR) spectroscopy. Recent applications of the TR-MFE technique have revealed its high potential for determining the hyperfine interaction (HFI) constants and the *g*-factors of radical ions in solutions.[5–13]

Hitherto, all the applications of TR-MFE have been restricted to radical ions having either magnetically equivalent nuclei or unresolved hyperfine structure. Hereafter the term "equivalent nuclei" means the nuclei having equal HFI constants with unpaired electron. Theory of TR-MFE in both the cases is well developed, and analytical expressions for spin evolution of radical pairs have been obtained and successfully applied to treat the experimental data.[3,11,14–17] Unfortunately, in many situations of experimental interest this theoretical treatment is not sufficient, since many radical ions with resolved EPR spectra may have nonequivalent magnetic nuclei. In the presence of nonequivalent nuclei, the solution of the problem at high magnetic field is not a difficult exercise,[3,14] but at zero field no exact analytical results for spin dynamics have been obtained so far. Since the solution for spin evolution at zero field is unknown, the TR-MFE kinetics cannot be evaluated. So far, only numerical simulations of MFE have been performed that encourage one to apply the TR-MFE technique for studying radical ions with nonequivalent magnetic nuclei.[6,16] However, to recognize clearly a potential of TR-MFE for studying such radical ions a more detailed analysis is required.

The present work is aimed at obtaining analytical results for TR-MFE in recombination fluorescence of radical-ion pairs, where one (or both) of the radical ions has either two magnetically nonequivalent nuclei or two groups of equivalent nuclei. The first group has n_1 spin I_1 nuclei with HFI constant a_1, while in the second group there are n_2 spin I_2 nuclei with HFI constant a_2. Theoretical results are applied to treat experimental TR-MFE curves obtained for three different radical-ion pairs containing radical cations of 2,3-

[a)]Author to whom correspondence should be addressed. Electronic mail: ivanov@tomo.nsc.ru

dimethylbutane, 2,2,6,6-tetramethylpiperidine, or diisopropylamine and radical anion of *p*-terphenyl-d_{14} (*p*TP).

II. THEORY

A. Basic principles of TR-MFE

In the TR-MFE experiment radiolytic impact on solution containing electron acceptors A and hole acceptors D rapidly produces radical-ion pairs (RIP) in their spin-correlated singlet state $^1[A^{\bullet-}\cdots D^{\bullet+}]$. A luminophor with sufficient fluorescence quantum yield and short fluorescence time τ_f is usually chosen as one of the charge acceptors. In nonpolar solution, RIP recombination is not spin selective and RIP recombines from both singlet and triplet states at the same rate but fluorescence is produced only from the singlet recombination product. Prior to its recombination, RIP may change its spin state due to HFI, difference in g-factors of radical ions and/or paramagnetic relaxation.

If fluorescent time τ_f is short enough, experimentally measured fluorescence intensity at external magnetic field B $I_B(t)$ obeys the following equation:[18]

$$I_B(t) = F(t)\left(\theta\rho_{SS}^B(t) + \tfrac{1}{4}(1-\theta)\right), \tag{2.1}$$

where $F(t)$ is the lifetime distribution of RIPs, θ is the fraction of recombining RIPs originating from the same precursor (geminate pairs), $\rho_{SS}^B(t)$ is the population of their singlet state. Equation (2.1) implies the same lifetime distributions for geminate and cross recombining RIPs. The accuracy of this assumption has been checked by Monte Carlo modeling of radical-ion recombination in multiparticle tracks.[19] The simulation revealed that the ratio of the recombination rates of geminate and cross recombining RIPs becomes time-independent after several picoseconds.

Knowing the time behavior of $\rho_{SS}(t)$ at high magnetic field B, one can obtain the EPR spectrum of the radical pair making Fourier transformation. Unfortunately, to evaluate this quantity from $I_B(t)$ the time dependence of recombination function $F(t)$ is required, which is unknown. To minimize this problem it is a common practice to measure the ratio of the fluorescence kinetics at high and zero magnetic fields. This quantity called the TR-MFE is as follows:

$$\mathrm{MFE}(t) = \frac{I_B(t)}{I_0(t)}. \tag{2.2}$$

In the simplest case, where fluorescence time τ_f is very short and RIPs under study are created instantly, the TR-MFE kinetics does not contain $F(t)$,

$$\mathrm{MFE}(t) = \frac{\theta\rho_{SS}^B(t) + \frac{1}{4}(1-\theta)}{\theta\rho_{SS}^0(t) + \frac{1}{4}(1-\theta)}. \tag{2.3}$$

For more rigorous analysis, it is necessary to take into account both finite τ_f and $F(t)$ dependence as well as finite setup response time and duration of pulsed generation of RIPs. In this case, expression for recombination fluorescence is recast as follows:

$$I_{0,B}(t) = \frac{1}{\tau_f}\int_{-\infty}^{t} d\tau \exp\left(-\frac{t-\tau}{\tau_f}\right)\int_{-\infty}^{\tau} d\xi F(\tau-\xi) \times\left\{\theta\rho_{SS}^{0,B}(\tau-\xi) + \tfrac{1}{4}(1-\theta)\right\}G(\xi). \tag{2.4}$$

Here we introduced $G(t)$ to account for the last two aforementioned factors. In the present work $G(t)$ was approximated as a rectangular shape function of time,

$$G(t) = \begin{cases} 1/t_g, & -t_g/2 < t < t_g/2 \\ 0, & |t| > t_g/2. \end{cases} \tag{2.5}$$

Note, the $F(t)$ value for geminate recombination of RIPs decreases rapidly at earlier time and becomes slow decaying at longer times. As a consequence, accounting the real $F(t)$ dependence is of importance only at short times $t \lesssim \tau_f$, t_g. In this work, the recombination function $F(t)$ was approximated as follows:

$$F(t) \propto \frac{1}{(t+t_0)^{3/2}}, \tag{2.6}$$

where the value of t_0 depends on the properties of the solvent and mobilities of the radical ions.

B. Evaluation of TR-MFE

Singlet state population of geminate RIP $\rho_{SS}^B(t)$ at arbitrary strength of external magnetic field can be written as follows:[15]

$$\rho_{SS}^B(t) = \tfrac{1}{4} - \mathrm{Tr}\{(\hat{\mathbf{S}}_1, \hat{\mathbf{S}}_2)\hat{\rho}(t)\}, \tag{2.7}$$

where $\hat{\rho}(t)$ is the density matrix of radical pair, $\hat{\mathbf{S}}_i = (\hat{S}_{ix}, \hat{S}_{iy}, \hat{S}_{iz})$ are electron spin operators of the first ($i=1$) and second ($i=2$) radicals. This formula can be rewritten in terms of the components of the tensors $T_{ik}^{(1,2)}(t)$ describing the evolution of spin operators[16] for each of the radicals,

$$\rho_{SS}^B(t) = \frac{1}{4} + \sum_{i,k} T_{ik}^{(1)}(t)T_{ik}^{(2)}(t), \tag{2.8}$$

where $i, k = x, y, z$ and

$$T_{ik}^{(1)} = \langle \mathrm{Tr}_e\{\hat{S}_{1i}(t)\hat{S}_{1k}(0)\}\rangle, \quad T_{ik}^{(2)} = \langle \mathrm{Tr}_e\{\hat{S}_{2i}(t)\hat{S}_{2k}(0)\}\rangle. \tag{2.9}$$

Here $\langle\cdots\rangle$ denotes the averaging over the nuclear spin states of radicals, trace is taken over electron spin states.

At high magnetic fields, i.e., $B \gg a_{eff}$, where a_{eff} is the effective HFI constant of radical pair secular approximation for HFI is applicable. As a consequence, solution of the problem is greatly simplified and analytical results for $\rho_{SS}^B(t)$ can be obtained. For example, for a RIP where one of the radical ions has two nuclei with even spins I_1 and I_2 having HFI constants a_1 and a_2, respectively, and the other has no HFI the solution for $\rho_{SS}^B(t)$ is as follows:[3,14]

$$\rho_{SS}^{B}(t)=\frac{1}{4}+\frac{\exp(-t/T_1)}{4}+\frac{\exp(-t/T_2)}{2(2I_1+1)(2I_2+1)}\cos\left(\frac{\Delta g\beta Bt}{\hbar}\right)\times\sum_{m_1=-I_1}^{I_1}\cos(m_1a_1t)\sum_{m_2=-I_2}^{I_2}\cos(m_2a_2t). \quad (2.10)$$

Here $\Delta g=g_1-g_2$ is the difference of radical g-factors. Paramagnetic spin relaxation is taken into account as well as the dynamic spin evolution for RIP, and T_1 and T_2 are the longitudinal and transverse relaxation times, respectively. For another frequently met situation where the first radical has n_1 spins $1/2$ nuclei with HFI constant a_1 and n_2 spins $1/2$ nuclei with HFI constant a_2 and the second radical has no HFI $\rho_{SS}^{B}(t)$ is of the form:[3,14]

$$\rho_{SS}^{B}(t)=\frac{1}{4}+\frac{\exp(-t/T_1)}{4}+\frac{\exp(-t/T_2)}{2}\left(\cos\frac{a_1t}{2}\right)^{n_1}\times\left(\cos\frac{a_2t}{2}\right)^{n_2}\cos\left(\frac{\Delta g\beta Bt}{\hbar}\right). \quad (2.11)$$

In a more general way the solution for $\rho_{SS}^{B}(t)$ at $B\gg a_{eff}$ can be presented as follows:[17]

$$\rho_{SS}^{B}(t)=\frac{1}{4}+\frac{\exp(-t/T_1)}{4}+\frac{\exp(-t/T_2)}{2}\sum_{i,k\neq z}T_{ik}^{(1)}(t)T_{ik}^{(2)}(t). \quad (2.12)$$

Tensor components $T_{ik}^{(1,2)}(t)$ can easily be calculated for *arbitrary* hyperfine structure of each of the radical ions.

In contrast to the high field case, at zero field the problem of calculating the spin tensor components is much more complicated. So far, only the cases of either *equivalent* magnetic nuclei[3,14,17] or *unresolved* HFI (Ref. 15) on each radical ion have been resolved analytically. The aim of the present work is to obtain analytical results for a more general case where the partners of RIP have two groups of magnetically equivalent nuclei. For the sake of clarity we evaluate the spin tensor components only for the first radical ion assuming that the second radical has no magnetic nuclei. This assumption is not of principal importance: one may take into account HFI of the electron spin with one or two groups of equivalent nuclei or with unresolved HFIs in the second radical ion as well. In terms of the spin Hamiltonian $\hat{\mathcal{H}}$ of the first radical the expression for $T_{ik}^{(1)}$ takes the form

$$T_{ik}^{(1)}=\frac{1}{N_{I_1I_2}}\mathrm{Tr}\{\exp(i\hat{\mathcal{H}}t)\hat{S}_{1i}\exp(-i\hat{\mathcal{H}}t)\hat{S}_{1k}\}. \quad (2.13)$$

Here trace is taken over both electron and nuclear spin states and the coefficient

$$N_{I_1I_2}=(2I_1+1)(2I_2+1) \quad (2.14)$$

provides normalization condition at $t=0$: $T_{ik}^{(1)}=\delta_{ik}/2$. Due to the absence of HFI in the second radical, at any instant of time $T_{ik}^{(2)}=\delta_{ik}/2$. At zero magnetic field the Hamiltonian $\hat{\mathcal{H}}$ of the first radical is as follows:

$$\hat{\mathcal{H}}=a_1(\hat{\mathbf{S}}_1,\hat{\mathbf{I}}_1)+a_2(\hat{\mathbf{S}}_1,\hat{\mathbf{I}}_2)=\hat{V}_1+\hat{V}_2. \quad (2.15)$$

It describes isotropic HFI of electron spin with either two nuclei having spins I_1 and I_2 with HFI constants a_1 and a_2, respectively, or with two groups of equivalent nuclei.

In the case of two groups of magnetically equivalent nuclei spins I_1 and I_2 can be treated as the total nuclear momenta of both groups. For instance, total momentum I of n protons varies from $1/2$ to $n/2$ (odd n) or from 0 to $n/2$ (even n) and the coefficients of the distribution over I are given by the formula[8]

$$P_{n,I}=\frac{(2I+1)^2n!}{2^n(n/2-I)!(n/2+I+1)!}. \quad (2.16)$$

As a consequence, in order to obtain the $T_{ik}^{(1)}$ one first should evaluate it from Eq. (2.13) in configuration with fixed total momenta I_1 and I_2 in these groups, since I_1 and I_2 are "good" quantum numbers because the total nuclear spin in each group obviously commutes with the radical spin Hamiltonian. Then the result should be averaged over I_1 and I_2 with appropriate weighting factors. For n spins $1/2$ the weighting factor is given by Eq. (2.16).

To calculate the desired quantities $T_{ik}^{(1)}$ we choose the following basis:

$$|JMj\rangle, \quad (2.17)$$

that is, the state with fixed total momentum $\hat{\mathbf{J}}=\hat{\mathbf{S}}_1+\hat{\mathbf{I}}_1+\hat{\mathbf{I}}_2$, its projection M on Z axis and total nuclear momentum $\hat{\mathbf{j}}=\hat{\mathbf{I}}_1+\hat{\mathbf{I}}_2$. Both J and M are good quantum numbers because the operators $\hat{\mathbf{J}}^2$ and $\hat{J}_z$ commute with the Hamiltonian $\hat{\mathcal{H}}$ (2.15). Although $[\hat{\mathbf{j}}^2,\hat{\mathcal{H}}]\neq 0$ and the Hamiltonian does not keep j constant the solution of the problem in the basis (2.17) is still feasible. Fortunately, at any J nuclear momentum j can be equal only to $J\pm 1/2$ (because $\hat{\mathbf{J}}=\hat{\mathbf{S}}_1+\hat{\mathbf{j}}$ and $S_1=1/2$). That is, at any J there are only two possible values of j. Therefore, the Hamiltonian splits into blocks 2×2.

As zero field it is sufficient to calculate only a single component $T_{zz}^{(1)}$ of the spin tensor for two reasons. First, $T_{xx}^{(1)}=T_{yy}^{(1)}=T_{zz}^{(1)}$ owing to the symmetry of the system (at zero field there is no preferred axis of quantization in space). Second, all the nondiagonal components of the tensors are equal to zero, e.g., $T_{zx}^{(1)}=T_{zy}^{(1)}=T_{xy}^{(1)}=0$. This is because the operators $\hat{S}_{1z}$, $\exp(i\hat{\mathcal{H}}t)$, $\exp(-i\hat{\mathcal{H}}t)$ keep constant the projection M of the total momentum J of three spins, while the action of operators $\hat{S}_{1x}$, $\hat{S}_{1y}$ change this projection to projection $M'=M\pm 1$, thus, the trace of product of these four operators vanishes. Indeed,

$$\begin{aligned}&\mathrm{Tr}\{\exp(i\hat{\mathcal{H}}t)\hat{S}_{1z}\exp(-i\hat{\mathcal{H}}t)\hat{S}_{1x}\}\\&=\sum_{J,M,j}\langle JMj|\exp(i\hat{\mathcal{H}}t)\hat{S}_{1z}\exp(-i\hat{\mathcal{H}}t)\hat{S}_{1x}|JMj\rangle\\&=\sum_{J,M,j}\sum_{J',j'}A_{Jj;J'j'}^{M}\langle J'Mj'|\hat{S}_{1x}|JMj\rangle=0.\end{aligned} \quad (2.18)$$

Here $A_{Jj;J'j'}^{M}$ is the coefficient dependent on J, J', j, j', M. Consequently, the result for $\rho_{SS}^{0}(t)$ (2.8) is as follows:

$$\rho_{SS}^{0}(t) = \tfrac{1}{4} + \tfrac{3}{2}T_{zz}^{(1)}(t). \tag{2.19}$$

The problem of calculating matrix elements of $\hat{\mathcal{H}}$ is similar to that of summing three momenta in quantum mechanics.[20,21] In the case under study these momenta $\hat{\mathbf{j}}_1$, $\hat{\mathbf{j}}_2$, and $\hat{\mathbf{j}}_3$ are as follows:

$$\hat{\mathbf{j}}_1 = \hat{\mathbf{S}}_1, \quad \hat{\mathbf{j}}_2 = \hat{\mathbf{I}}_1, \quad \hat{\mathbf{j}}_3 = \hat{\mathbf{I}}_2. \tag{2.20}$$

To calculate matrix elements of $\hat{\mathcal{H}}$ we shall introduce the notations for sums of momenta following Refs. 20 and 21,

$$\hat{\mathbf{j}}_{12} = \hat{\mathbf{j}}_1 + \hat{\mathbf{j}}_2 = \hat{\mathbf{S}}_1 + \hat{\mathbf{I}}_1,$$

$$\hat{\mathbf{j}}_{13} = \hat{\mathbf{j}}_1 + \hat{\mathbf{j}}_3 = \hat{\mathbf{S}}_1 + \hat{\mathbf{I}}_2,$$

$$\hat{\mathbf{j}}_{23} = \hat{\mathbf{j}}_2 + \hat{\mathbf{j}}_3 = \hat{\mathbf{I}}_1 + \hat{\mathbf{I}}_2 = \hat{\mathbf{j}}. \tag{2.21}$$

Let us now calculate the elements of $\hat{V}_1$ and $\hat{V}_2$ that constitute the Hamiltonian. Matrix elements of $\hat{V}_1$ should first be calculated in the basis with fixed momentum j_{12}: $|JMj_{12}\rangle = |j_{12}\rangle$ and then transformed to those in basis (2.17). The value of j_{12} varies from $|I_1 - 1/2|$ to $I_1 + 1/2$. It is bound with the initial basis (2.17) by the following relation:[20,21]

$$\langle JMj_{23}|JMj_{12}\rangle = \langle j_{23}|j_{12}\rangle = (-1)^{I_1+I_2+J+1/2}\sqrt{(2j_{12}+1)(2j_{23}+1)} \times \begin{Bmatrix} \frac{1}{2} & I_1 & j_{12} \\ I_2 & J & j_{23} \end{Bmatrix}, \tag{2.22}$$

where

$$\begin{Bmatrix} j_1 & j_2 & j_3 \\ j_4 & j_5 & j_6 \end{Bmatrix}$$

denotes the Racah $6j$-symbol. Operator $\hat{V}_1$ can be rewritten as follows:

$$\hat{V}_1 = \frac{a_1}{2}(\hat{\mathbf{j}}_{12}^2 - \hat{\mathbf{I}}_1^2 - \hat{\mathbf{S}}_1^2). \tag{2.23}$$

In the basis of its eigenfunctions $|JMj_{12}\rangle$ its elements can easily be calculated,

$$\langle JMj_{12}|\hat{V}_1|JMj_{12}\rangle = \frac{a_1}{2}\left[j_{12}(j_{12}+1) - I_1(I_1+1) - \tfrac{3}{4}\right]. \tag{2.24}$$

As a consequence, elements of $\hat{V}_1$ in basis (2.17) take the form

$$\langle JMj_{23}|\hat{V}_1|JMj'_{23}\rangle = \frac{a_1}{2}\sum_{j_{12}=|I_1-1/2|}^{I_1+1/2}\left[j_{12}(j_{12}+1) - I_1(I_1+1) - \tfrac{3}{4}\right]\langle j_{23}|j_{12}\rangle\langle j_{12}|j'_{23}\rangle. \tag{2.25}$$

Similarly, to determine the elements of $\hat{V}_2$ we shall first specify them in its eigenbasis $|JMj_{13}\rangle = |j_{13}\rangle$,

$$\langle JMj_{13}|\hat{V}_2|JMj_{13}\rangle = \frac{a_2}{2}\left[j_{13}(j_{13}+1) - I_2(I_2+1) - \tfrac{3}{4}\right]. \tag{2.26}$$

which is bound with basis (2.17) by the following relation:[20,21]

$$\langle JMj_{23}|JMj_{13}\rangle = \langle j_{23}|j_{13}\rangle = (-1)^{J+j_{23}+1/2}\sqrt{(2j_{13}+1)(2j_{23}+1)} \times \begin{Bmatrix} \frac{1}{2} & I_2 & j_{13} \\ I_1 & J & j_{23} \end{Bmatrix}. \tag{2.27}$$

Here the sign (power of -1) is introduced in a different way as compared to Eq. (2.22). This is not a mistake or a misprint but a correct result of momenta summation because the sign of the spin wave function depends on the order in which the spins are summed.[20,21] Second, similar to Eq. (2.25) we rewrite the elements of $\hat{V}_2$ in basis (2.17) as follows:

$$\langle JMj_{23}|\hat{V}_2|JMj'_{23}\rangle = \frac{a_2}{2}\sum_{j_{13}=|I_2-1/2|}^{I_2+1/2}\left[j_{13}(j_{13}+1) - I_2(I_2+1) - \tfrac{3}{4}\right]\langle j_{23}|j_{13}\rangle\langle j_{13}|j'_{23}\rangle. \tag{2.28}$$

As has been mentioned above at any J we have to specify only four elements of $\hat{\mathcal{H}}$:

$$\mathcal{H}_{11}(J) = \langle JM, J-\tfrac{1}{2}|\hat{\mathcal{H}}|JM, J-\tfrac{1}{2}\rangle,$$

$$\mathcal{H}_{12}(J) = \langle JM, J-\tfrac{1}{2}|\hat{\mathcal{H}}|JM, J+\tfrac{1}{2}\rangle,$$

$$\mathcal{H}_{21}(J) = \langle JM, J+\tfrac{1}{2}|\hat{\mathcal{H}}|JM, J-\tfrac{1}{2}\rangle,$$

$$\mathcal{H}_{22}(J) = \langle JM, J+\tfrac{1}{2}|\hat{\mathcal{H}}|JM, J+\tfrac{1}{2}\rangle, \tag{2.29}$$

which are independent of the projection M of the total momentum in full accordance with the Wigner–Eckart theorem[20] for the elements of scalar products. Performing summation in Eqs. (2.25) and (2.28) we obtain the following results for these elements:

$$\mathcal{H}_{11}(J) = -\frac{a_1+a_2}{4} + \gamma_J\frac{a_1+a_2}{8} + \alpha_J\beta_J\gamma_J\frac{a_1-a_2}{8},$$

$$\mathcal{H}_{22}(J) = -\frac{a_1+a_2}{4} - \gamma_J\frac{a_1+a_2}{8} - \alpha_J\beta_J\gamma_J\frac{a_1-a_2}{8},$$

$$\mathcal{H}_{12}(J) = \mathcal{H}_{21}(J) = \gamma_J\frac{a_1-a_2}{8}\sqrt{\beta_J^2-1}\sqrt{1-\alpha_J^2}. \tag{2.30}$$

Here we introduced new quantities,

$$\alpha_J = 2\frac{I_1-I_2}{2J+1}, \quad \beta_J = 2\frac{I_1+I_2+1}{2J+1}, \quad \gamma_J = 2J+1. \tag{2.31}$$

At given I_1 and I_2 total momentum J varies from $||I_1-I_2| - 1/2|$ to $I_1+I_2+1/2$. To evaluate tensor components (2.13)

we have to obtain the expressions for the matrix exponents of the Hamiltonian, i.e., the following matrices:

$$\hat{A}_J(t) = \exp\left[i\begin{pmatrix} \mathcal{H}_{11}(J) & \mathcal{H}_{12}(J) \\ \mathcal{H}_{12}(J) & \mathcal{H}_{22}(J) \end{pmatrix} t \right] = \begin{pmatrix} f_J & h_J \\ h_J & g_J \end{pmatrix},$$

$$\hat{B}_J(t) = \exp\left[-i\begin{pmatrix} \mathcal{H}_{11}(J) & \mathcal{H}_{12}(J) \\ \mathcal{H}_{12}(J) & \mathcal{H}_{22}(J) \end{pmatrix} t \right] = \begin{pmatrix} f_J^* & h_J^* \\ h_J^* & g_J^* \end{pmatrix}, \tag{2.32}$$

where "$*$" denotes complex conjugate value. The quantities f_J, g_J, h_J can be easily calculated:

$$f_J = e^{i\lambda_J^+ t}\frac{1+\cos\theta_J}{2} + e^{i\lambda_J^- t}\frac{1-\cos\theta_J}{2}$$
$$= e^{i\lambda_J^+ t}\cos^2\frac{\theta_J}{2} + e^{i\lambda_J^- t}\sin^2\frac{\theta_J}{2},$$

$$g_J = e^{i\lambda_J^+ t}\frac{1-\cos\theta_J}{2} + e^{i\lambda_J^- t}\frac{1+\cos\theta_J}{2}$$
$$= e^{i\lambda_J^+ t}\sin^2\frac{\theta_J}{2} + e^{i\lambda_J^- t}\cos^2\frac{\theta_J}{2},$$

$$h_J = \frac{\sin\theta_J}{2}(e^{i\lambda_J^+ t} - e^{i\lambda_J^- t}), \tag{2.33}$$

where

$$\lambda_J^{\pm} = -\frac{a_1+a_2}{4} \pm \frac{\sqrt{D_J}}{2} \tag{2.34}$$

are the egenvalues of the Hamiltonian at given J,

$$\theta_J = \arcsin\left(\frac{2\mathcal{H}_{12}(J)}{\sqrt{D_J}}\right) \tag{2.35}$$

is the "mixing angle" of states $|JM, J-1/2\rangle$ and $|JM, J+1/2\rangle$ and

$$D_J = [\mathcal{H}_{11}(J) - \mathcal{H}_{22}(J)]^2 + 4\mathcal{H}_{12}^2(J) = \gamma_J^2\frac{(a_1+a_2)^2 + (a_1-a_2)^2(\alpha_J^2+\beta_J^2-1) + 2(a_1^2-a_2^2)\alpha_J\beta_J}{16}$$
$$= \frac{a_1-a_2}{4}[(2I_1+1)^2 a_1 - (2I_2+1)^2 a_2] + \frac{a_1 a_2}{4}(2J+1)^2. \tag{2.36}$$

Elements of $\hat{S}_{1i}$ required for evaluation of tensor (2.13) can be expressed via the components of the so-called irreducible tensors $f_{k,q}$ in the following way:

$$f_{1,0} = i\hat{S}_{1z}, \quad f_{1,\pm 1} = \mp\frac{i}{\sqrt{2}}(\hat{S}_{1x} \pm \hat{S}_{1y}). \tag{2.37}$$

As has been mentioned above we restrict ourselves to calculating only the elements of $\hat{S}_{1z} = -if_{1,0}$. Elements of $f_{1,0}$ in basis (2.17) are of the form[20] of the Hamiltonian, i.e., the following matrices:

$$\langle J'M'j'|f_{1,0}|JMj\rangle = i\cdot\delta_{jj'}\delta_{MM'}$$
$$\times(-1)^{\mathcal{J}_{\max}-M}\begin{pmatrix} J' & 1 & J \\ -M & 0 & M \end{pmatrix}$$
$$\times\langle J'j||f_{1,0}||Jj\rangle. \tag{2.38}$$

Here

$$\begin{pmatrix} j_1 & j_2 & j_3 \\ m_1 & m_2 & m_3 \end{pmatrix}$$

is the Wigner $3j$-symbol, $\mathcal{J}_{\max} = \max\{J, J'\}$ and $\langle J'j||f_{1,0}||Jj\rangle$ is the so-called reduced element of the tensor $f_{1,0}$, which is as follows[20]

$$\langle J'j||f_{1,0}||Jj\rangle = (-1)^{j+\mathcal{J}_{\min}+3/2}\sqrt{2J+1}\sqrt{2J'+1}$$
$$\times\begin{Bmatrix} \frac{1}{2} & J' & j \\ J & \frac{1}{2} & 1 \end{Bmatrix}\langle j||f_{1,0}||j\rangle$$
$$= (-1)^{j+\mathcal{J}_{\min}+3/2}\sqrt{\frac{3}{2}}\sqrt{2J+1}\sqrt{2J'+1}$$
$$\times\begin{Bmatrix} \frac{1}{2} & J' & j \\ J & \frac{1}{2} & 1 \end{Bmatrix}. \tag{2.39}$$

Here $\mathcal{J}_{\min} = \min\{J, J'\}$. As a result, we arrive at the expression for $\hat{S}_{1z}$ elements,

$$\langle J'M'j'|\hat{S}_{1z}|JMj\rangle = \delta_{jj'}\delta_{MM'}$$
$$\times(-1)^{j+3/2-M}\sqrt{\frac{3}{2}}\sqrt{2J+1}\sqrt{2J'+1}$$
$$\times\begin{pmatrix} J' & 1 & J \\ -M & 0 & M \end{pmatrix}\begin{Bmatrix} \frac{1}{2} & J' & j \\ J & \frac{1}{2} & 1 \end{Bmatrix}. \tag{2.40}$$

Finally, we can obtain the following expression for $T_{zz}^{(1)}$ at given J and M:

$$T_{zz}^{(1)}(J,M,t)=\frac{1}{N_{I_1I_2}}\sum_{J'=J-1}^{J+1}\sum_{j=J-1/2}^{J+1/2}\sum_{j'=J-1/2}^{J+1/2}\langle JMj|\hat{A}_J|JMj'\rangle\langle JMj'|\hat{S}_{1z}|J'Mj'\rangle\langle J'Mj'|\hat{B}_{J'}|J'Mj\rangle\langle J'Mj|\hat{S}_{1z}|JMj\rangle$$

$$=\frac{1}{N_{I_1I_2}}\sum_{J'=J-1}^{J+1}\sum_{j'=J-1/2}^{J+1/2}\sum_{j'=J-1/2}^{J+1/2}\langle JMj|\hat{A}_J|JMj'\rangle\langle J'Mj'|\hat{B}_{J'}|J'Mj'\rangle\frac{3}{2}(-1)^{j+j'-2M+1}(2J+1)(2J'+1)$$

$$\times\begin{pmatrix}J' & 1 & J\\ -M & 0 & M\end{pmatrix}^2\begin{Bmatrix}\frac{1}{2} & J' & j\\ J & \frac{1}{2} & 1\end{Bmatrix}\begin{Bmatrix}\frac{1}{2} & J & j'\\ J' & \frac{1}{2} & 1\end{Bmatrix}. \tag{2.41}$$

Here summation over J' is from $J-1$ to $J+1$ because the action of $\hat{S}_{1z}$ on spin state with fixed J results in total momentum $J'=J-1$, J, $J+1$. Performing summation in Eq. (2.41) we obtain the following expression for $T_{zz}^{(1)}(J,M,t)$:

$$N_{I_1I_2}T_{zz}^{(1)}(J,M,t)=\frac{f_J}{4}\left(g_{J-1}^*\frac{J^2-M^2}{J^2}+f_J^*\frac{M^2}{J^2}\right)+\frac{g_J}{4}\left(f_{J+1}^*\frac{(J+1)^2-M^2}{(J+1)^2}+g_J^*\frac{M^2}{(J+1)^2}\right)-\frac{h_Jh_J^*}{2}\frac{M^2}{J(J+1)}. \tag{2.42}$$

Performing summation over all possible M (from $-J$ to J) and keeping in mind that

$$\sum_{M=-J}^{J}M^2=\frac{J(J+1)(2J+1)}{3}$$

we arrive at the following result for $T_{zz}^{(1)}$ at fixed J:

$$N_{I_1I_2}T_{zz}^{(1)}(J,t)=f_Jf_J^*\frac{(J+1)(2J+1)}{12J}+g_Jg_J^*\frac{J(2J+1)}{12(J+1)}-h_Jh_J^*\frac{2J+1}{6}+f_Jg_{J-1}^*\frac{4J^2-1}{12J}+g_Jf_{J+1}^*\frac{4(J+1)^2-1}{12(J+1)}. \tag{2.43}$$

Total value of $T_{zz}^{(1)}$ component of the spin tensor can be obtained by summation of this quantity from $J=J_{\min}=||I_1-I_2|-1/2|$ to $J=J_{\max}=I_1+I_2+1/2$, i.e.,

$$T_{zz}^{(1)}(t)=\sum_{J=J_{\min}}^{J_{\max}}T_{zz}^{(1)}(J,t). \tag{2.44}$$

At $J=J_{\max}=I_1+I_2+1/2$ both $g_{J_{\max}}$ and $h_{J_{\max}}$ vanish (because j cannot be equal to $J_{\max}+1/2$) and $f_{J_{\max}}=1$. At $J=J_{\min}$ there are two possibilities. If $I_1\neq I_2$ both $f_{J_{\min}}$ and $h_{J_{\min}}$ vanish and $g_{J_{\min}}=1$. If $I_1=I_2$ both $f_{J_{\min}}$ and $h_{J_{\min}}$ do not vanish at $J=J_{\min}$. Finally, at $J_{\min}<J<J_{\max}$ all three quantities f_J, g_J, h_J exist.

Keeping this in mind, we can recast Eq. (2.43) in a simpler way. First, if all three quantities f_J, g_J, h_J exist at given J, one can obtain the following result using their definitions given by Eq. (2.33),

$$f_Jf_J^*\frac{(J+1)(2J+1)}{12J}+g_Jg_J^*\frac{J(2J+1)}{12(J+1)}-h_Jh_J^*\frac{2J+1}{6}=\frac{(2J+1)^3}{12J(J+1)}\cdot\frac{\sin^2\theta_J}{2}(\cos\sqrt{D_J}t-1)+(2J+1)\frac{(J+1)^2+J^2}{12J(J+1)}. \tag{2.45}$$

Expression for the real part of the quantity $f_Jg_{J-1}^*$ can be written as follows:

$$\begin{aligned}\mathrm{Re}\{f_Jg_{J-1}^*\}&=\cos(\lambda_J^+-\lambda_{J-1}^+)t\cos^2\frac{\theta_J}{2}\sin^2\frac{\theta_{J-1}}{2}+\cos(\lambda_J^+-\lambda_{J-1}^-)t\cos^2\frac{\theta_J}{2}\cos^2\frac{\theta_{J-1}}{2}\\&+\cos(\lambda_J^--\lambda_{J-1}^+)t\sin^2\frac{\theta_J}{2}\sin^2\frac{\theta_{J-1}}{2}+\cos(\lambda_J^--\lambda_{J-1}^-)t\sin^2\frac{\theta_J}{2}\cos^2\frac{\theta_{J-1}}{2}\\&=\cos\left(\frac{\sqrt{D_J}-\sqrt{D_{J-1}}}{2}t\right)\frac{1-\cos\theta_J\cos\theta_{J-1}}{2}+\cos\left(\frac{\sqrt{D_J}+\sqrt{D_{J-1}}}{2}t\right)\frac{1+\cos\theta_J\cos\theta_{J-1}}{2}.\end{aligned} \tag{2.46}$$

Then, denoting the coefficient of $f_Jg_{J-1}^*$ in Eq. (2.43) as K_J and that of $g_Jf_{J+1}^*$ as K_J' we obtain

$$K_J=\frac{4J^2-1}{12J}=K_{J-1}',\quad K_J'=\frac{4(J+1)^2-1}{12(J+1)}=K_{J+1}. \tag{2.47}$$

This means that $T_{zz}^{(1)}(J-1,t)$ and $T_{zz}^{(1)}(J+1,t)$ contain terms conjugate to the last two terms in the expression for $T_{zz}^{(1)}(J,t)$ (2.43). This allows us to recast the results for $T_{zz}^{(1)}$ [Eqs. (2.43) and (2.44)]. At $I_1\neq I_2$,

$$T_{zz}^{(1)}(t) = \frac{(J_{\max}+1)(2J_{\max}+1)}{12J_{\max}N_{I_1I_2}} + \frac{J_{\min}(2J_{\min}+1)}{12(J_{\min}+1)N_{I_1I_2}} + \frac{1}{N_{I_1I_2}}\sum_{J=J_{\min}+1}^{J_{\max}} \frac{4J^2-1}{12J}\left\{\cos\left(\frac{\sqrt{D_J}-\sqrt{D_{J-1}}}{2}t\right)\times(1-\cos\theta_J\cos\theta_{J-1}) + \cos\left(\frac{\sqrt{D_J}+\sqrt{D_{J-1}}}{2}t\right)\times(1+\cos\theta_J\cos\theta_{J-1})\right\} + \frac{1}{N_{I_1I_2}}\sum_{J=J_{\min}+1}^{J_{\max}-1}\left(\frac{(2J+1)^3}{12J(J+1)}\cdot\frac{\sin^2\theta_J}{2}\times(\cos\sqrt{D_J}t-1) + (2J+1)\frac{(J+1)^2+J^2}{12J(J+1)}\right), \quad (2.48)$$

while at $I_1=I_2$,

$$T_{zz}^{(1)}(t) = \frac{(J_{\max}+1)(2J_{\max}+1)}{12J_{\max}N_{I_1I_2}} + \frac{1}{N_{I_1I_2}}\sum_{J=J_{\min}+1}^{J_{\max}} \frac{4J^2-1}{12J}\left\{\cos\left(\frac{\sqrt{D_J}-\sqrt{D_{J-1}}}{2}t\right)\times(1-\cos\theta_J\cos\theta_{J-1}) + \cos\left(\frac{\sqrt{D_J}+\sqrt{D_{J-1}}}{2}t\right)\times(1+\cos\theta_J\cos\theta_{J-1})\right\} + \frac{1}{N_{I_1I_2}}\sum_{J=J_{\min}}^{J_{\max}-1}\left(\frac{(2J+1)^3}{12J(J+1)}\cdot\frac{\sin^2\theta_J}{2}(\cos\sqrt{D_J}t-1) + (2J+1)\frac{(J+1)^2+J^2}{12J(J+1)}\right). \quad (2.49)$$

General expressions (2.48) and (2.49) are still relatively cumbersome because arbitrary spins I_1 and I_2 are considered. Nonetheless, their use is preferable for simulating the TR-MFE curves, since the purely numerical calculation of the TR-MFE becomes very time-consuming for systems with high spin nuclei or large number of nuclei. For particular values of I_1 and I_2, expressions (2.48) and (2.49) become much simpler. For $I_1=I$, $I_2=1/2$, and $I_1=I$, $I_2=1$ they are given in the Appendix.

To treat the experimental data for TR-MFE it is also necessary to take into consideration the paramagnetic spin relaxation at zero field, like it has been done for the high field in Eqs. (2.10)–(2.12), i.e., to modify formula (2.19). Here we do this in the following rather simple way:

$$\rho_{SS}^0(t) = \tfrac{1}{4} + \tfrac{3}{2}T_{zz}^{(1)}(t)\exp(-t/T_0). \quad (2.50)$$

Here T_0 is an effective paramagnetic relaxation time at zero magnetic field. This means of taking into account the spin relaxation at zero field gives rather accurate results for TR-MFE as has been demonstrated in a number of works.[8,11–13] For more rigorous consideration of relaxation, the knowledge of particular relaxation mechanism is required.

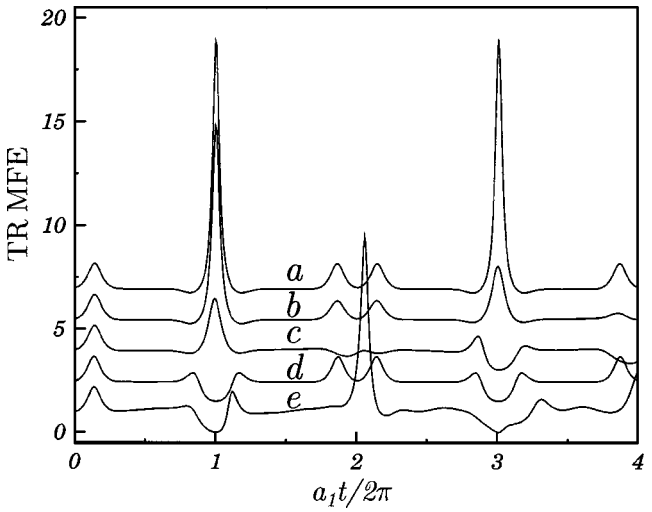

FIG. 1. Model calculations of TR-MFE kinetics for RIP where one of the partners has no HFI and the other one has $n_1=12$ spin 1/2 nuclei with HFI constant a_1 and one spin 1/2 nucleus with HFI constant a_2 equal to 0 (a); $0.1a_1$ (b); $0.5a_1$ (c); a_1 (d); $-a_1$ (e). Here we neglect paramagnetic relaxation, contribution of nongeminate pairs to MFE, difference of g-factors of radicals, finite fluorescence time, and delay in formation of RIPs. For convenience, the curves are arbitrarily shifted along the vertical.

C. Model calculations of the TR-MFE in the presence of nonequivalent nuclei

By means of formulas (2.12) and (2.50) it is relatively easy to calculate the TR-MFE for RIP containing radical ion with two groups of equivalent nuclei. As has been emphasized above, the quantum beats in recombination fluorescence have shown that the TR-MFE is a perspective technique for studying radical ions with nonequivalent nuclei.[7,12,13] In particular, numerical simulations revealed that the TR-MFE could be sensitive to the relative signs of the HFI constants.[13] This statement is supported by Eq. (2.48) and (2.49), in which the frequencies of oscillations dictated by D_J (2.36) are dependent on the values of both $(a_1+a_2)^2$ and $(a_1-a_2)^2$. To illustrate the features of TR-MFE in the case of two groups of nonequivalent nuclei, we shall perform simulations based on the foregoing theoretical results. For the sake of simplicity here we completely neglect the difference in g-factors of radical ions, paramagnetic relaxation and contribution of nongeminate RIPs to recombination fluorescence, and focus our attention solely on the HFI-induced quantum beats in recombination fluorescence.

To demonstrate how the TR-MFE is affected by the presence of nonequivalent magnetic nuclei we have considered two examples.

In the first example, we start with a RIP comprising the first radical ion with even number $n_1=12$ of spin 1/2 equivalent nuclei with HFI constant a_1 and the second radical ion with no magnetic nuclei. In this case the TR-MFE [see Fig. 1, curve (a)] is known to be periodic function (period $T=4\pi/a_1$) with characteristic sequence of stronger and weaker peaks.[8] As has been shown earlier[8] in the limit of large n_1 the shape and position of the first peak is reproduced also in the so-called semiclassical model of Schulten *et al.*[15] where the individual HFI constants are assumed to be nonresolved. Thus, this peak will later on be referred to as the Schulten's peak.

Now let us add to the first radical one more spin 1/2 nucleus with the HFI constant a_2. If a_2 is small in comparison with a_1 the positions of peaks in the TR-MFE curve remain the same, however, their intensities decrease with time [Fig. 1, curve (b)]. Thus, adding an extra nucleus with small HFI constant is similar to inhomogeneous broadening of the radical EPR lines. If a_2 is comparable with a_1 the TR-MFE curve becomes strongly distorted [Fig. 1, curve (c)]: the positions and intensities of peaks are noticeably changed and even troughs appear instead of some peaks. Note the Schulten's peak position remains nearly the same. If $a_2=a_1$ we obtain the well-known TR-MFE curve[8] for odd number of magnetically equivalent spin 1/2 nuclei [Fig. 1, curve (d)]. In this case, the curve is again periodic as for even number of equivalent spin 1/2 nuclei [curve (a)]. However, the strong peak at $t=2\pi/a_1$ is replaced by a well-pronounced trough. Finally, let us take $a_2=-a_1$. As is readily seen from Fig. 1, curve (e) addition of nonequivalent nucleus with HFI constant $a_2=-a_1$ distorts the time behavior of $\rho_{SS}^0(t)$, in particular, violates its periodicity. In this case the high-field fluorescence kinetics

$$I_B(t)=\rho_{SS}^B(t)F(t)=\frac{F(t)}{2}\left\{1+\left(\cos\frac{a_1 t}{2}\right)^{n_1+1}\right\} \qquad (2.51)$$

as well as the high-field EPR spectrum of RIP are exactly the same as in the case of $a_2=a_1$, i.e., they are not sensitive to the relative sign of HFI constants a_1 and a_2. At zero field the situation is qualitatively different. This is because the energies of the RIP eigenstates given by Eq. (2.34) are sensitive to relative sign of a_1 and a_2. For $a_2=a_1$ the function $\rho_{SS}^0(t)$ is periodic and its period is equal to $T=4\pi/a_1$, while for $a_2=-a_1$ the function is a combination of oscillating sine and cosine functions with the frequencies whose ratios are, generally speaking, irrational. As a result, the periodicity both of $\rho_{SS}^0(t)$ and TR-MFT curve is violated.

The second example, as shown in Fig. 2, concerns the case where two nuclei with spins 1/2 and 1 have the same or opposite sings of HFI constants: $a_1=a_2$ and $a_1=-a_2$. It is clearly seen from Fig. 2(a) that spin dynamics at the high field is exactly the same for both cases and is not sensitive to the relative signs of the HFI constants. To the contrary, $\rho_{SS}^0(t)$ [Fig. 2(b)] and TR-MFE [Fig. 2(c)] in these situations differ drastically. Particularly, intensive peak in $\rho_{SS}^0(t)$ curve at $t=4\pi/a_1$ turns into a trough when one goes from the case $a_1=a_2$ to $a_1=-a_2$ [Fig. 2(b)]. As a consequence, rather strong peak appears in the TR-MFE curve at this instant of time [Fig. 2(c)].

These simulations clearly demonstrate that the TR-MFE technique is very sensitive to nonequivalence of magnetic nuclei, in particular, to relative signs of the HFI constants. While the absolute values of the HFI constants can usually be determined by the conventional EPR spectroscopy, their signs are often unknown. In this case, the TR-MFE technique can be very useful for determining the relative HFI signs.

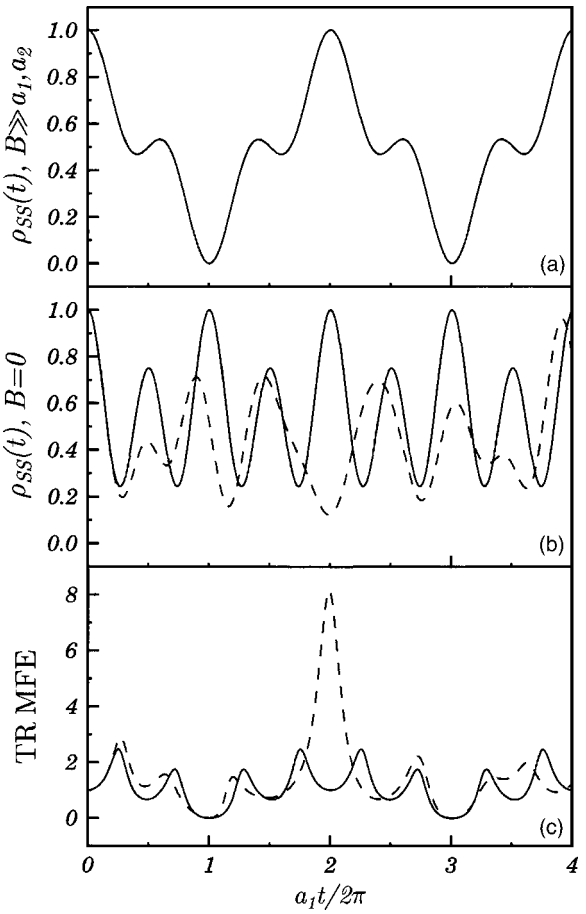

FIG. 2. Model calculations of RIP singlet state population at high (a) and zero (b) magnetic fields and TR-MFE kinetics (c) for RIP where one of partners has no HFI and the other has two nuclei with spins 1/2 and 1. HFI constant of the nuclei have the same absolute values but either same signs $a_1=a_2$ (solid lines) or opposite signs $a_1=-a_2$ (dashed lines). Here we neglect paramagnetic relaxation, contribution of nongeminate pairs to MFE, difference of g factors of radicals, finite fluorescence time, and delay in formation of RIPs.

This encourages us to apply this method to radical ions with nonequivalent nuclei. The examples given below demonstrate that the fitting of the experimental TR-MFE curves with the formulas (2.4), (2.12), and (2.50) provide reliable extraction of the HFI constants from experimental data.

III. EXPERIMENT

The delayed fluorescence of studied solutions was detected by single photon counting technique using an x-ray fluorimeter described elsewhere.[22] The duration of the ionizing pulse was less than 2 ns. The light was collected using an optical bandpass filter (260–390 nm) to separate the fluorescence of *para*-terphenyl (*p*TP). Strong magnetic field was 0.1 ± 0.005 T. Zero magnetic field was adjusted to within 0.05 mT.

n-Hexane and *c*-hexane used as solvents were stirred with concentrated sulfuric acid, washed with water, distilled

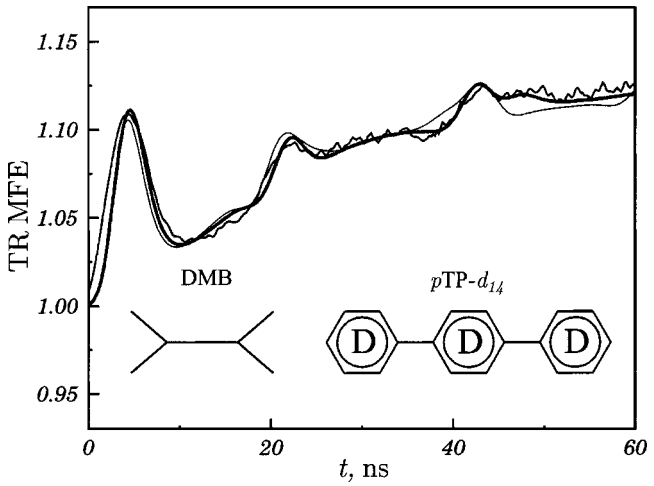

FIG. 3. TR-MFE curves (scatter plot) obtained in solution of 0.1M DMB and 30 μM of *p*TP in *n*-hexane. Thick line shows the best fit of experimental kinetics obtained with the following parameters: $a_1=a(12H)=1.66$ mT, $a_2=a(2H)=0.65$ mT, $\theta=0.13$, $T_0=20$ ns, $T_1=2000$ ns, $T_2=20$ ns, $t_g=1$ ns, $t_0=1$ ns, $\tau_f=1.2$ ns. Thin line shows the best simulation with different relative sign of a_1 and a_2, where we obtained $a_1=a(12H)=1.77$ mT, $a_2=a(2H)=-0.68$ mT, $\theta=0.125$, all the rest parameters are the same as in the simulation with $\mathrm{sgn}(a_1)=\mathrm{sgn}(a_2)$.

over sodium, and passed through a 0.5 m column of activated alumina three times. 2,3-dimethylbutane (Fluka, 99%) (DMB) was processed with the same procedure except for stirring with sulfuric acid. With the gas chromatography we revealed that *n*-hexane available contained 2-methylpentane (0.2%) and 3-methylpentane (0.6%) as the main impurities. These alkane isomers could not be removed with the purification method used but their presence was believed not to affect the experimental findings. The concentration of unsaturated hydrocarbon impurities was less than 10 ppm.

2,2,4,4-tetramethylpiperidine (99%) (TMPP), diisopropylamine (99%) (DIPA), and *para*-terphenyl-d_{14} (99%) were received from Aldrich. Amines were distilled before use. The solutions were degassed by repeated freeze-pump-thaw cycles. All measurements were made at 293 ± 0.5 K.

IV. RESULTS AND DISCUSSION

Here we present the experimental results for three systems and make a tight comparison of these results with the theory developed in the preceding section aimed at definition of HFI properties of elusive radical ions in nonpolar solutions. In all the cases presented in this section the HFI in radical cation can be modeled by two groups of equivalent nuclei. Special attention is paid in demonstrating the sensitivity of the TR-MFE curves to relative sings of HFI constants.

A. Radical-ion pair DMB$^{\bullet+}$/*p*TP$^{\bullet-}$

The experimental TR-MFE kinetics presented in Fig. 3 as a noisy line was obtained using solution 0.1M of DMB and 30 μM of *p*TP in *n*-hexane. In solution primary radical cations of the solvent molecules are captured by DMB molecules because of the lower value of its ionization potential.[23] It is likely that the rate of hole capture is controlled by diffusion and is about 3×10^{10} $\mathrm{M}^{-1}\,\mathrm{s}^{-1}$.[24] Excess electrons in studied solution are scavenged by only *p*TP with the rate constant of approximately 10^{12} $\mathrm{M}^{-1}\,\mathrm{s}^{-1}$.[25] Thus, the delayed fluorescence in the solution arises from recombination of pairs DMB$^{\bullet+}$/*p*TP$^{\bullet+}$ and the RIP spin dynamics is conditioned by HFIs in radical cations of DMB because HFI constants in perdeuterated *p*TP radical anions are rather small (the total effective HFI constant is 0.068 mT[26]). Our calculations show that the TR-MFE traces in the pair (as well as for the other two experimental systems under study) are not sensitive to spin dynamics of *p*TP in the time range 0–100 ns, thereby, fitting experimental data one can neglect the *p*TP HFI. The time delay in formation of the radical anions does not significantly affect the observed TR-MFE because excess electrons are not coupled to any magnetic nuclei.

In addition to the Schulten's peak with its maximum placed at 4–5 ns there are two damped peaks at 22 and 40 ns on the TR-MFE curve. The shape of these features differs drastically from that expected for a RIP, where the spin dynamics is conditioned merely by HFI with equivalent magnetic nuclei.[8,11] This observation is in qualitative agreement with presumptive hyperfine structure of DMB$^{\bullet+}$: there are two equivalent CH-protons and 12 equivalent protons of methyl groups. Equivalence of protons in each group is provided by fast rotation of the methyl groups and fast conformational transitions in the radical cation.[11] Accordingly, the TR-MFE curves (solid lines in Fig. 3) have been calculated under an assumption of two groups of equivalent protons on DMB$^{\bullet+}$. The best fit (thick line in Fig. 3) was obtained with HFI constants of the methyl group protons $a_1=a(12H)=1.66$ mT and those for the CH-protons $a_2=a(2H)=0.65$ mT. Important to note that these values of HFI constants are consistent with quantum chemical calculations.[27] Other simulation parameters are listed in the figure caption. Taking $\mathrm{sgn}(a_1)\neq\mathrm{sgn}(a_2)$, we make the agreement between the theory and the experiment noticeably worse (thin line in Fig. 3). The best fit for $\mathrm{sgn}(a_1)\neq\mathrm{sgn}(a_2)$ that gives $a_1=1.77$ and $a_2=-0.68$ mT accurately reproduces the first and the second maxima in the experimental TR-MFE observed at $t\approx4.5$ and $t\approx22$ ns, respectively, while at longer times the differences between the experimental and the simulated curves becomes greater: the features at $t\approx43$ ns are not reproduced properly by this simulation.

DMB$^{\bullet+}$ has earlier been observed by the EPR technique only in low temperature freon matrices.[28] Its EPR spectrum was determined by HFI with four equivalent protons of methyl groups with HFI constants of 3.8–4.5 mT.[28] The value of a_1 obtained in the present work for the protons of methyl groups is in good agreement with this result. When methyl groups rotation becomes allowed at higher temperatures, the number of the protons with nonzero spin density is to be tripled with accompanying threefold decrease of the HFI constant values. There are no reliable data on HFI constants with the CH-protons in matrices. From the low temperature EPR data it is expected that these HFI constants are much smaller as compared to those of the methyl groups protons.

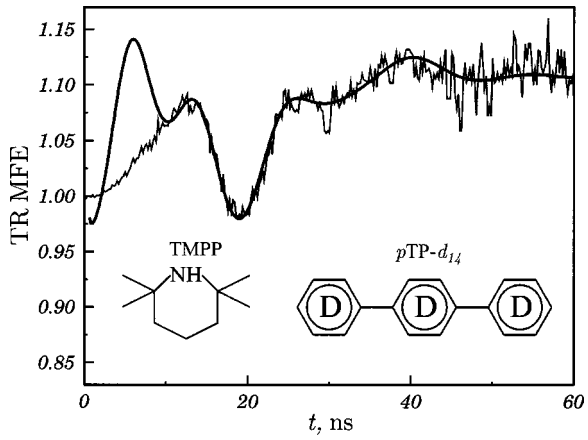

FIG. 4. TR-MFE curves (scatter plot) obtained in solution of 3 mM TMPP and 30 μM of *p*TP in *c*-hexane. Solid line shows the best fit of experimental kinetics obtained with the following parameters: $a_1=a(1H)=-1.85$ mT, $a_2=a(1N)=1.78$ mT, $\theta=0.18$, $T_0=12.3$ ns, $T_1=5000$ ns, $T_2=12.3$ ns, $t_g=1$ ns, $t_0=1$ ns, $\tau_f=1.2$ ns.

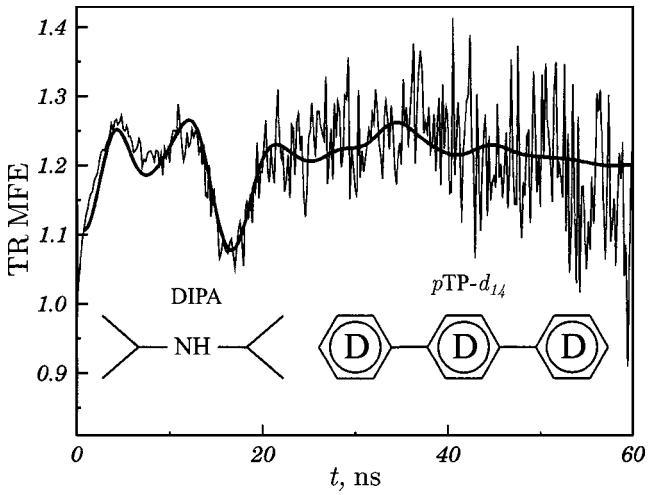

FIG. 5. TR-MFE curves (scatter plot) obtained in solution of 3 mM DIPA and 1 mM of *p*TP in *c*-hexane. Solid line shows the best fit of experimental kinetics obtained with the following parameters: $a_1=a(2H)=a(N)=2.1$ mT, $a_2=a(H)=-2.4$ mT, $\theta=0.22$, $T_0=15.4$ ns, $T_1=60$ ns, $T_2=15.4$ ns, $t_g=1$ ns, $t_0=1$ ns, $\tau_f=1.2$ ns.

It is important to emphasize that Trifunac *et al.*[29] doubt that $DMB^{\bullet+}$ radical cations exist in solution. However, in the present work this radical cation has been observed in solution at a room temperature by using the TR-MFE technique.

B. Radical-ion pair $TMPP^{\bullet+}/pTP^{\bullet-}$ in *c*-hexane

To study TMPP radical cation, we use the solution 3 mM TMPP+30 μM *p*TP in *c*-hexane. Rather low concentration of TMPP were chosen to diminish the contribution of diffusion encounters of $TMPP^{\bullet+}$ with TMPP molecules. We have found that at higher TMPP concentration encounters of $TMPP^{\bullet+}$ and TMPP lead to the formation of new radical cation species, presumably dimer radical cations $TMPP_2^{\bullet+}$. In general, this reaction pathway is well-known for radical cations of aliphatic amines.[30] Experimental work focused on identifying these species is now in progress.

In *c*-hexane the primary radical cations have very high mobility[31] resulting in high rate constant of secondary radical cation formation ($\sim 3\times 10^{11}$ M^{-1} s^{-1}). Due to this fact it is plausible that RIPs $TMPP^{\bullet+}/pTP^{\bullet-}$ are instantly born at $t=0$.

In Fig. 4 the experimental TR-MFE curve is shown as scatter plot. Thick line shows TR-MFE curve for $a_1=a(1H)=-1.85$ mT, $a_2=a(1N)=1.78$ mT. Other simulation parameters are listed in the figure caption. This simulation gives a good agreement of theoretical and experimental kinetics except for the region $t<10$ ns. The reason of the discrepancy is additional fluorescence of excited $TMPP^{*}$ and pTP^{*} molecules formed by energy transfer from singlet excited *c*-hexane molecules.[32] The contribution of this process to the measured fluorescence is significant during the first several nanosecond after ionizing pulse and it completely masks the Shulten's peak. It is likely that negative sign of the α-proton $a(1H)$ as obtained from our simulation arises due to spin polarization mechanism.[33]

Changing the relative HFI signs we can fit the experimental TR-MFE almost equally well with $a(1N)=1.81$ mT and $a(1H)=2.17$ mT. However, this can be done only by taking unreasonably short T_0 relaxation time equal to 5.4 ns. Therefore, we believe that the fit with $\mathrm{sgn}(a_1)\neq\mathrm{sgn}(a_2)$ is more reliable than that with $\mathrm{sgn}(a_1)=\mathrm{sgn}(a_2)$. Unfortunately, we cannot give a more convincing proof of $\mathrm{sgn}(a_1)\neq\mathrm{sgn}(a_2)$ within the experimental accuracy: the difference between simulations with different relative signs of HFI constants becomes more pronounced at long times, whereas in our experiments the signal/noise ratio decays with time. In the case under study this ratio at $t>30$ ns is too low to discriminate between the two simulations with different relative HFI signs.

C. Radical-ion pair $DIPA^{\bullet+}/pTP^{\bullet-}$ in *c*-hexane

As has been found by using the optically detected EPR radical cation of DIPA has four magnetic nuclei with the following HFI constants: $a(2H)=1.8$ mT, $a(1H)=2.15$ mT, and $a(N)=1.87$ mT.[34] Unfortunately, the optically detected EPR technique does not allow one to determine the signs of HFI constants but only their absolute values. $DIPA^{\bullet+}$ radical cation has also been studied by TR-MFE in $DIPA^{\bullet+}/pTP^{\bullet-}$ system.[8] However, in this work all the nuclei were considered equivalent with the HFI constant of 2.1 mT. Under these assumptions a relatively poor fit of the experimental MFE kinetics has been obtained. We believe that this is because the basic assumption of four equivalent nuclei is wrong, since the HFI constant of α-proton is presumably negative due to spin polarization mechanism,[33] while all the rest HFI constants should be positive. Therefore, here we reconsider the fitting of experimental results taking $a(1H)$ as a fitting parameter and assuming that the β-protons and nitrogen are magnetically equivalent nuclei with HFI constants $a(2H)=a(N)=2.1$ mT. The best fit of the experimental MFE kinetics has been obtained with $a(1H)=-2.4$ mT (Fig. 5, solid

line). Like in the previous case of TMPP the HFI constant of the α-proton is negative. If we then change the sign of $a(1H)$ we can attain good agreement between theoretial and experimental kinetics only by taking extremely short relaxation time $T_0=6.9$ ns, while T_2 is 20.3 ns. The HFI costants in the best fit are then $a(2H)=a(N)=2.2$ mT and $a(1H)=2.4$ mT. However, physically this very short T_0 is not reasonable for $DIPA^{\bullet+}$ radical cation, therefore, we believe that the HFI constant $a(1H)$ is negative. Unfortunately, to determine more clearly whether $a(1H)$ is positive or negative the experimental signal/noise ratio at $t>20$ ns is insufficient.

V. CONCLUSIONS

In the present work for the first time we obtained analytical solution for the time-resolved magnetic field kinetics for radical-ion pair with radicals containing two groups of magnetically equivalent nuclei. We believe that this solution is very useful for analyzing experimental TR-MFE curves and extracting the HFI constants from them. Our model calculations reveal that the TR-MFE kinetics are very sensitive to nonequivalence of the nuclei and to the relative signs of the HFI constants in two groups of equivalent nuclei.

Application of the present theory to three experimental systems (radical cation)/pTP$^{\bullet-}$ in alkane solutions confirm the efficiency of the method. By simulating the experimental TR-MFE traces we managed to obtain the data on the values and relative signs of HFI constants of radical cations.

ACKNOWLEDGMENTS

This work was supported by RFBR (Grant Nos. 05-03-32620, 05-03-32370), the program of Leading Science Schools (Grant No. NSh-84.2003.3), Russian Ministry of High Education (Grant No. 2298.2003.3). The authors are grateful to Professor P. A. Purtov for valuable comments on this work.

APPENDIX A: EXPRESSIONS FOR THE SPIN TENSOR

Here we present the result of the general formulas (2.48) or (2.49) for two particular cases (a) $I_1=I>1/2$ and $I_2=1/2$; (b) $I_1=I>1$ and $I_2=1$.

In case (a) the maximal total spin $J_{\max}$ is equal to $I+1$, while $J_{\min}=I-1$ and $N_{I_1I_2}=2(2I+1)$. Substituting $I_1=I$ and $I_2=1/2$ into general expressions, we obtain the following result for $T_{zz}^{(1)}(t)$:

$$T_{zz}^{(1)}(t)=\frac{(I+2)(2I+3)}{12(I+1)(2I+1)}+\frac{(I-1)(2I-1)}{12I(2I+1)}+\frac{2}{2I+1}\sum_{J=I}^{I+1}K_J\,\mathrm{Re}\{f_J g_{J-1}^{*}\}+\frac{(2I+1)^2}{12I(I+1)}\frac{\sin^2\theta_I}{2}(\cos\sqrt{D_I}t-1)+\frac{(I+1)^2+I^2}{12I(I+1)}. \tag{A1}$$

Substituting the value of $\mathrm{Re}\{f_J g_{J-1}^{*}\}$ from Eq. (2.46) we obtain

$$\begin{aligned}T_{zz}^{(1)}(t)=&\frac{2I^2+2I+1}{12I(I+1)}+\frac{(2I+1)^2}{24I(I+1)}\frac{\sin^2\theta_I}{2}(\cos\sqrt{D_I}t-1)\\&+\frac{2I+3}{12(I+1)}\left[\sin^2\frac{\theta_I}{2}\cos(\lambda_{I+1}-\lambda_I^{+})t+\cos^2\frac{\theta_J}{2}\cos(\lambda_{I+1}-\lambda_I^{-})t\right]\\&+\frac{2I-1}{12I}\left[\cos^2\frac{\theta_I}{2}\cos(\lambda_{I-1}-\lambda_I^{+})t+\sin^2\frac{\theta_I}{2}\cos(\lambda_{I-1}-\lambda_I^{-})t\right].\end{aligned} \tag{A2}$$

Here

$$\lambda_{I+1}=\frac{2Ia_1+a_2}{4},\quad \lambda_{I-1}=\frac{-2(I+1)a_1+a_2}{4}, \tag{A3}$$

$\lambda_I^{\pm}$ are given by Eq. (2.34), θ_I by Eq. (2.35) and D_I by Eq. (2.36).

For case $I_1=I$ and $I_2=1$ the values of J can be equal to $J_{\min}=I-3/2, I-1/2, I+1/2, I+3/2=J_{\max}$ and the normalization factor $N_{I_1I_2}$ is as follows:

$$N_{I_1I_2}=3(2I+1). \tag{A4}$$

From general expression (2.48) the following result for $T_{zz}^{(1)}\times(t)$ can be obtained:

$$\begin{aligned}N_{I_1I_2}T_{zz}^{(1)}(t)=&\frac{(I+2)(2I+5)}{6(2I+3)}+\frac{(I-1)(2I-3)}{6(2I-1)}\\&+2\sum_{J=I-1/2}^{I+3/2}K_J\,\mathrm{Re}\{f_J g_{J-1}^{*}\}\\&+\sum_{J=I-1/2}^{I+1/2}\left(\frac{(2J+1)^2}{12J(J+1)}\frac{\sin^2\theta_J}{2}\cos\sqrt{D_J}t+\frac{(J+1)^2+J^2}{12J(J+1)}\right).\end{aligned} \tag{A5}$$

Substituting $\mathrm{Re}\{f_J g_{J-1}^{*}\}$ from Eq. (2.46) we arrive at the following expression:

$$N_{I_1I_2}T^{(1)}_{zz}(t) = \frac{2I+1}{2} + \frac{4I}{3(4I^2-1)} + \frac{1}{3(2I+3)} + \frac{4I^3}{3(4I^2-1)}\sin^2\theta_-(\cos\sqrt{D_{I-1/2}}t - 1) + \frac{4(I+1)^3}{3(2I+1)(2I+3)}\sin^2\theta_+(\cos\sqrt{D_{I+1/2}}t - 1)$$
$$+ \frac{4I(I-1)}{3(2I-1)}\left[\cos^2\frac{\theta_-}{2}\cos(\lambda^+_{I-1/2} - \lambda_{I-3/2})t + \sin^2\frac{\theta_-}{2}\cos(\lambda^-_{I-1/2} - \lambda_{I-3/2})t\right] + \frac{4(I+1)(I+2)}{3(2I+3)}\left[\sin^2\frac{\theta_+}{2}\cos(\lambda^+_{I+1/2}\right.$$
$$\left. - \lambda_{I+3/2})t + \cos^2\frac{\theta_+}{2}\cos(\lambda^-_{I-1/2} - \lambda_{I+3/2})t\right] + \frac{2I(I+1)}{3(2I+1)}\left[\cos\left(\frac{\sqrt{D_{I+1/2}} + \sqrt{D_{I-1/2}}}{2}t\right)(1 + \cos\theta_+\cos\theta_-)\right.$$
$$\left. + \cos\left(\frac{\sqrt{D_{I+1/2}} - \sqrt{D_{I-1/2}}}{2}t\right)(1 - \cos\theta_+\cos\theta_-)\right]. \quad \text{(A6)}$$

Here

$$\lambda_{I+3/2} = \frac{a_2 + Ia_1}{2}, \quad \lambda_{I-3/2} = \frac{a_2 - (I+1)a_1}{2}. \quad \text{(A7)}$$

Eigenvalues $\lambda^{\pm}_{I\pm1/2}$, mixing angles

$$\theta_+ = \theta_{I+1/2}, \quad \theta_- = \theta_{I-1/2}, \quad \text{(A8)}$$

and the quantities $D_{I\pm1/2}$ are given by Eqs. (2.34)–(2.36), respectively.

[1] B. Brocklehurst, Faraday Discuss. Chem. Soc. **63**, 96 (1977).
[2] J. Klein and R. Voltz, Can. J. Chem. **55**, 2102 (1977).
[3] K. M. Salikhov, Yu. N. Molin, R. Z. Sagdeev, and A. L. Buchachenko, *Spin Polarization and Magnetic Effects in Chemical Reactions* (Akademiai Kiado, Budapesht, 1984).
[4] A. V. Veselov, V. I. Melekhov, O. A. Anisimov, and Yu. N. Molin, Chem. Phys. Lett. **136**, 263 (1987).
[5] O. M. Usov, V. M. Grigoryantz, B. M. Tadzhikov, and Yu. N. Molin, Radiat. Phys. Chem. **49** 237 (1997).
[6] B. Brocklehurst, J. Chem. Soc., Faraday Trans. **93**, 1079 (1997).
[7] Yu. N. Molin, Bull. Korean Chem. Soc. **20**, 7 (1999).
[8] V. A. Bagryansky, O. M. Usov, V. I. Borovkov, T. V. Kobzeva, and Yu. N. Molin, Chem. Phys. **255**, 237 (2000).
[9] V. I. Borovkov, V. A. Bagryansky, I. V. Yeletskikh, and Yu. N. Molin, Mol. Phys. **100**, 1379 (2002).
[10] V. I. Borovkov, V. A. Bagryansky, Yu. N. Molin, M. P. Egorov, and O. M. Nefedov, Phys. Chem. Chem. Phys. **5**, 2027 (2003).
[11] V. A. Bagryansky, V. I. Borovkov, and Yu. N. Molin, Phys. Chem. Chem. Phys. **6**, 924 (2004).
[12] Yu. N. Molin, Mendeleev Commun. No. 3, 85 (2004).
[13] B. Brocklehurst, Chem. Soc. Rev. **31**, 301 (2002).
[14] B. Brocklehurst, J. Chem. Soc., Faraday Trans. 2 **72**, 1869 (1976).
[15] K. Schulten and P. G. Wolynes, J. Chem. Phys. **68**, 3292 (1978).
[16] E. W. Knapp and K. Schulten, J. Chem. Phys. **71**, 1978 (1979).
[17] V. O. Saik, N. N. Lukzen, V. M. Grigoryants, O. A. Anisimov, A. B. Doktorov, and Yu. N. Molin, Chem. Phys. **84**, 421 (1984).
[18] S. V. Anishchik, V. I. Borovkov, V. I. Ivannikov, I. V. Shebolaev, Yu. D. Chernousov, N. N. Lukzen, O. A. Anisimov, and Yu. N. Molin, Chem. Phys. **242**, 319 (1999).
[19] V. V. Lozovoy, S. V. Anishchik, N. N. Medvedev, O. A. Anisimov, and Yu. N. Molin, Chem. Phys. Lett. **167**, 122 (1999).
[20] L. D. Landau and E. M. Lifshits, *Quantum Mechanics* (Nauka, Moscow, 1963).
[21] D. A. Varshalovich, A. N. Moskalev, and V. K. Hersonsky, *Quantum Theory of Angular Momentum* (Nauka, Leningrad, 1975).
[22] S. V. Anishchik, V. M. Grigoryantz, I. V. Shebolaev, Yu. D. Chernousov, O. A. Anisimov, and Yu. N. Molin, Prib. Tekh. Eksp. **4**, 74 (1989).
[23] Webbook, Internet interface to NIST databases, http://webbook.nist.gov
[24] V. I. Borovkov, Chem. Phys. Lett. **394**, 441 (2004).
[25] L. G. Christophorou, Z. Phys. Chem. (Munich) **195**, 195 (1996).
[26] A. Berndt, L. Grossi, M. T. Jones, M. Lehnig, and L. Lunazzi, in *Numerical Data and Functional Relationship in Science and Technology*, edited by H. Fisher, Landolt-Börnstein New Series, Group II, Vol. 17f (Springer, Berlin, 1990).
[27] L. N. Shchegoleva, private communication, unpublished results.
[28] K. Toriyama, in *Radical Ionic Systems. Properties in Condensed Phases*, edited by A. Lund and M. Shiotani (Kluwer Academic, Dordrecht, 1991), pp. 99–124, and references therein.
[29] D. W. Werst and A. D. Trifunac, J. Phys. Chem. **92**, 1093 (1988).
[30] J. C. Scaiano, S. Garcia, and H. Garcia, Tetrahedron Lett. **34**, 5929 (1997).
[31] I. A. Shkrob, M. C. Sauer, K. H. Schmidt, A. D. Ziu, J. Yan, and A. D. Trifunac, J. Phys. Chem. **101**, 2120 (1997).
[32] M. C. Sauer, Jr., C. D. Jonah, and C. A. Naleway, J. Phys. Chem. **95**, 730 (1991).
[33] A. Carrington and A. D. McLachlan, *Introdution to Magnetic Resonance with Applications to Chemistry and Chemical Physics* (Harper & Row, New York, 1967), paragraph 6.4.
[34] D. W. Werst and A. D. Trifunac, J. Phys. Chem. **95**, 1268 (1991).